Session B4: *fiN*, rN Reactions

Chairman: H. L. ANDERSON

Organizer: W. LEE

Scientific Secretaries: Y. WATANABE
N. SASAO

1. Photoproduction at SPS, I
——Emulsion Experiments
G. DIAMBRINI-PALAZZI
2. Photoproduction at SPS, II
——<£, p_9 p^r Photoproductions and Search for Charmed Meson
A. KEMP
3. Photoproduction at FNAL, I
——Total Cross Section and <*fi* Photoproduction
D. O. CALDWELL
4. Photoproduction at FNAL, II
——Search for Charm
W. LEE
5. Muon Proton Scattering Experiments at FNAL, I
R. WILSON
6. *fz—p* Scattering Experiment at FNAL, II
K. W. CHEN
7. Neutral Kaon Form Factors
B. WlNSTEIN
8. Charged Kaon Form Factors
E. N. TSYGANOV

(Thursday, August 24, 1978; 14: 50-17: 20)

PROC. 19th INT. CONF. HIGH ENERGY PHYSICS
TOKYO, 1978

B 4 Preliminary Results of a Search for Charmed Particles Photoproduced in Nuclear Emulsions Coupled with the OMEGA System of CERN

Presented by G. DIAMBRINI-PALAZZI

Photon Emulsion Collaboration and Omega Photon Collaboration

We present here the preliminary results of an experiment on charm photoproducton in nuclear emulsions coupled with the CERN magnetic spectrometer OMEGA, using the 80 GeV tagged bremsstrahlung beam from the CERN-SPS. The experiment[1,2] represents a new approach to the experimental problem of determining the life-time of charm particles. In fact, the use of a photon reaction has an important advantage with respect to a neutrino induced reaction because, while the ratio between the charm and total photoproduction cross sections $a_c/a_t c \wedge l0^{\sim 2}$ is not far from the analogous value for the neutrino interactions, the o_c value is about seven orders of magnitude larger for photons than for neutrinos. A possible disadvantage could be the electromagnetic background produced in the emulsion, but this has been circumvented by using a new exposure technique.[1,2]

Secondaries from photohadronic events in the emulsion were detected by OMEGA, a combined system of spark chambers, MWPC, drift chambers and a Cerenkov threshold counter.[3]

Six hundred emulsions of size 144 x 66 X 0.6 mm^3 have been exposed. They were driven into position one at a time by a pneumatic device and were exposed at an angle of 11° with the beam to a dose of about 2x 10^6 photons *(i.e.,* about 10 SPS bursts). In this way, the electromagnetic background in the emulsion was kept to an acceptably low level.

For each selected event the interaction vertex was reconstructed and those localized in the emulsion were searched for within an area of 77 mm^2. Up to now, 482 photohadronic events have been found within the tagged-photon energy range 20^-80 GeV, showing tracks with emission angles consistent with those recontructed by OMEGA.

Track following was performed on all the matched events, up to a maximum distance of 3 mm from the vertex. Concerning the results, no charm candidate event has been observed between 30 and 3000 *jum* from the main vertex. Instead, some trident-like events have been observed at distance between 10 and 30 *jam.*

The ability of this experiment to detect charm decays can be defined as the product $p\{r) \cdot e(r)$ of the probability $p(r)$ that a charm particle with lifetime r decays inside the emulsion thickness times the observability

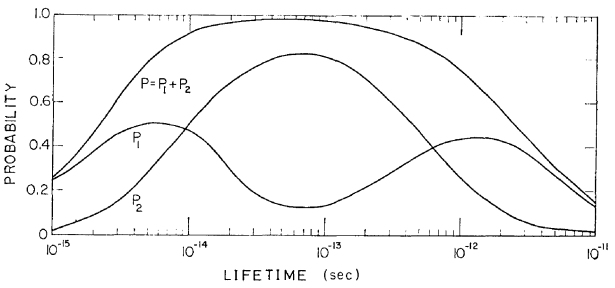

Fig. 1. Decay probability in the range 5-3000 /*um* for pairs of short lived particles as a function of the mean lifetime. The curves labelled *pi* and p_2 are related to the detection of only one, or both particles.

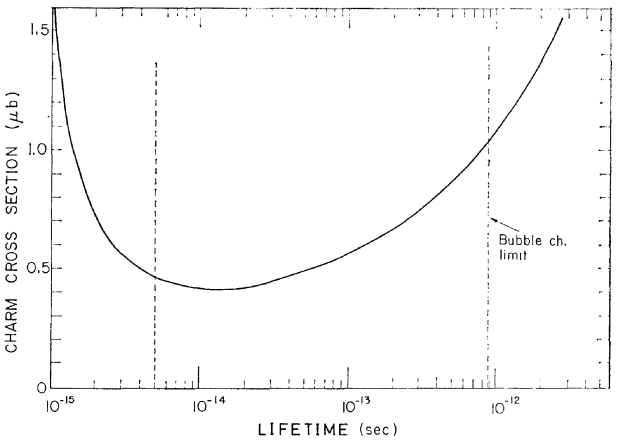

Fig. 2. 90% confidence level limit on pair production of short lived particles by 20-70 GeV photons in the emulsion.

s(r) of such a decay in the emulsion. Both these functions were estimated with a Monte-Carlo program.

A phenomenological inclusive dependence of charm photoproduction[4] has been assumed. The range within which a charm decay could be detected, is assumed to be from 5 up to 3000 /urn from the main vertex. According to this model, the probabilities p_u p_2 of detecting only one or both of the charm decays are given as a function of the lifetime r. It can be seen in Fig. 1 that between 10"[14] and 10"[12] sec the total probability $p=p_x+p_2$ lies between 0.8 and 1, while outside this range $Pi>P*$.

If we assume that no charm decay is seen in the 5-3000 /um range then the upper limit of the charm cross section value at the 90% confidence level, is given by the curve in Fig. 2. While the charm photoproduction cross section has not been measured so far, both indirect experimental evidence[5] and theoretical predictions[6] seem to suggest a value of the order of 1 /ub in our energy range. By taking these values and not regarding our candidates as charms we see from Fig. 2 that the charm lifetime must be either longer than 10~~[12] sec or shorter than 1.5-10"[15] sec at the 90% con-

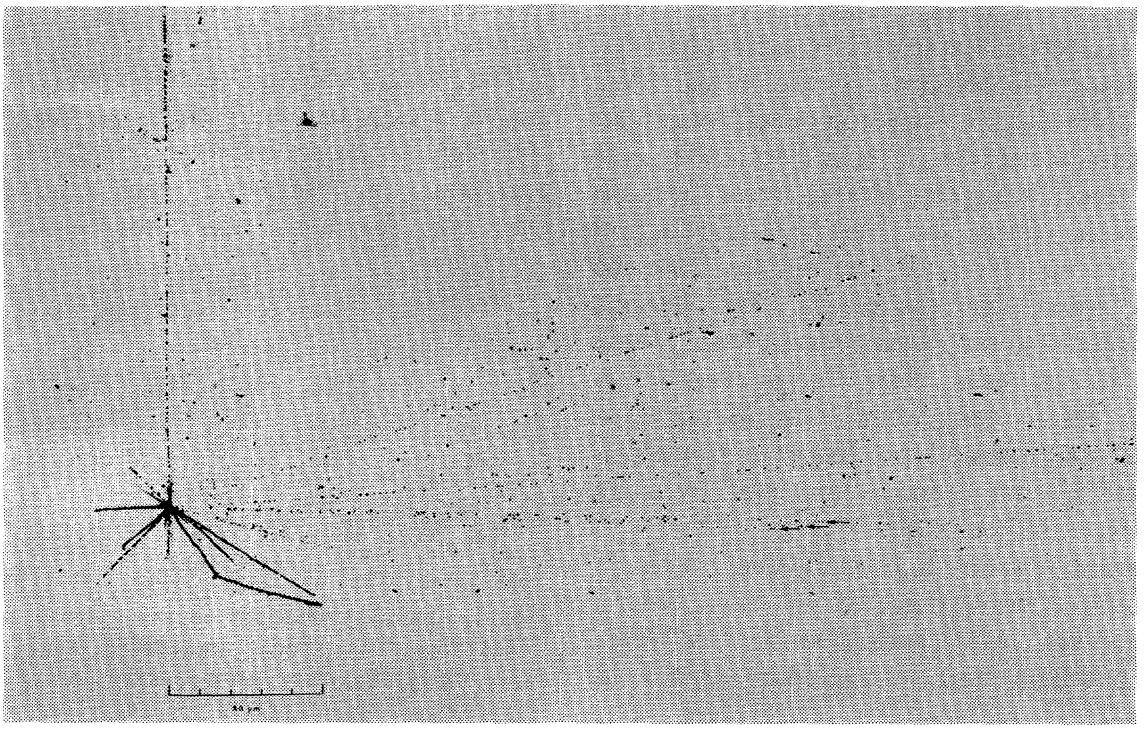

Fig. 3. Photomicrograph of a nuclear star produced by a 64 GeV photon coming from the left. A trident-like secondary event is shown by the arrows. A possible hyperfragment decay is visible.

Table I. Trident-like events

Event	Decay path (μm)	Photon energy (GeV)	Tracks Charge momentum (GeV/c)	Angular aperture (deg)	Invariant mass[e] (GeV/c^2)	Decay time (sec)
a)	16±3	64.1	1)[a] +23.913 2)[a] + 7.759 3)[a] − 7.899	3.4±.2	$M(\pi, \pi, \pi)=1.1\pm.2$	0.2×10^{-14}
b)	30±2	65.1	1)[a] +37.452 2)[a,b] − 0.800 3)[a,b] −0.100—0.500	6±0.2	$M(K, \pi, e,)=\sim1.2\pm.2$	0.46×10^{-14}

[a] Charge and momentum obtained by Omega.
[b] Tentative association for track (2); track (3) is probably an electron, its momentum limits are evaluated by multiple scattering measurements.
[e] About missing neutral particles see the text.

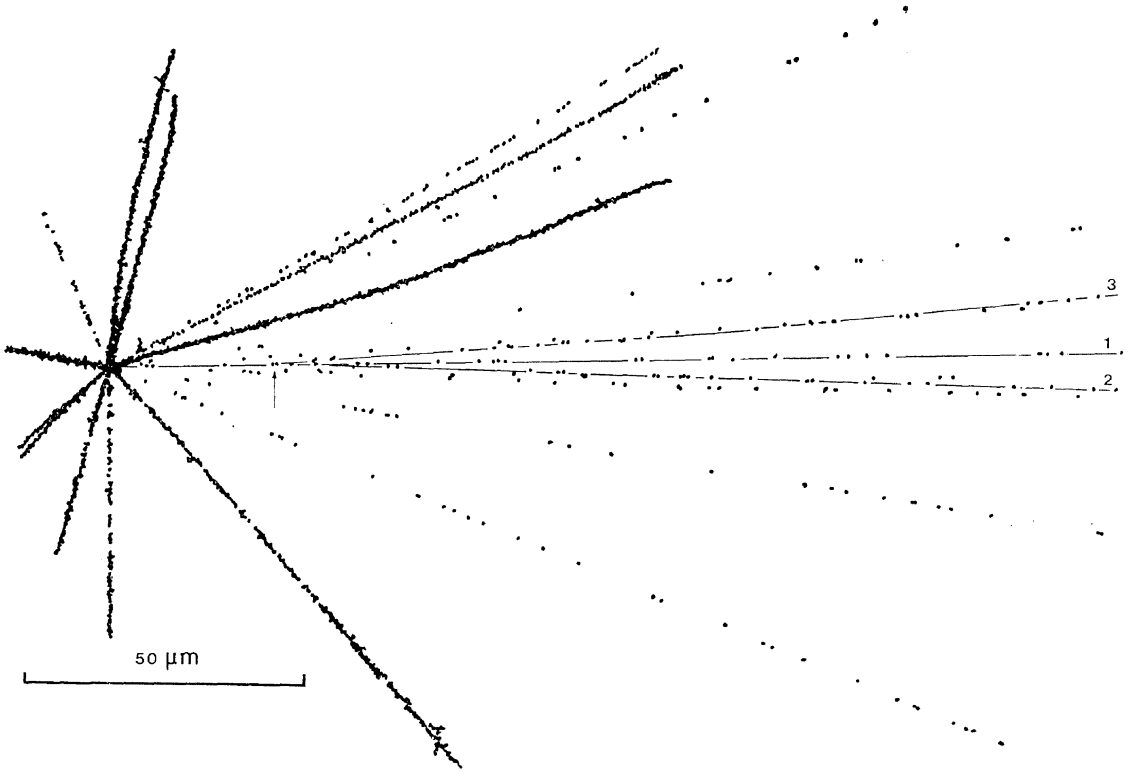

Fig. 4. Micrograph of a nulcear star produced by a 65 GeV photon coming from the left. The presence of the trident, whose parameters are listed in Table I section b), is made clearer by dotted lines.

fidence level. Furthermore, taking into account the upper limit given by bubble chamber experiments,[7] the charm lifetime should not be longer than 1.5-10~[15] sec.

The previous conclusions have been drawn following the assumptions that no candidate for charm decay had been seen. Actually, a few possible events have been observed in the range 10-30 /um from the main vertex, which could be interpreted as short-lived particle decays, like charms, with a decaytime of 0.2-*-0.5 X 10~[14] sec. The main experimental difficulty in observing these events is due to the small-angle aperture of decay products, together with rather short decay paths.

The event (a) of table I is a trident (see Fig. 3) with a calculated intersection point at 16.4;±3 *am* from the main vertex. This value is the combined result of 4 independent measurements. All the tracks of the trident are very well matched so that their momenta are unambiguously known as well as related Cerenkov signals, and tagged photon energy. For this trident, the Cerenkov signals are consistent with assumption that tracks (2), (3) are pions, while track (1) could be a pion or a kaon. Therefore a possible charmed meson interpretation of this event is D^+->K°7r$^+$;r$^+$7r~ because the *AS=AC* rule forbids a decay like D^+->K^+7r$^+$;r~. Invariant mass could be around 1.9 GeV, taking into account the unseen K°.

The trident (b) of Table I was found in one of the first few matched events from a recent exposure; its measurement is not completed. The aperture of the outer tracks is ~6^0±.2 and the decay path is 30±2 /urn. Track (1) (see Fig. 4) is associated with a positive high-energy track in OMEGA withp=37.5 GeV/c. Track (2) has been tentatively associated with a negative OMEGA track with /?=0.800 GeV/c_9 while the third one, unseen in OMEGA, is probably a low energy electron as it undergoes a rather large multiple scattering. Attributing a negative charge to the latter, a possible charm interpretation of this trident is the semileptonic decay:

$$D^- \rightarrow K^+ + \pi^- + e^- + \nu.$$

The decay time corresponding to these events is 2-*-5x 10~[15] sec, which is a factor 20-50 shorter than the theoretical central value.

The fact that we observe only one particle of the charmed pair is in agreement with the

ratio $pi/p_2=4$ in the range 2-5 x 10~[15] sec of mean life, as well as with the assumption of associated charmed meson baryon photoproduction.

The cross section corresponding to these two trident-like events is ~0.5 *ph.*

Alternatively, if we disregard such events and if we assume the theoretically expected value for the lifetime to be right, say 7x 10"[13] sec,[8] then we conclude from our data (see Fig. 2) that the charm photoproduction cross-section must be lower than 1 */ab.*

References

1. CERN/SPSC/74-29; SPSC/P-10, April 1974.
2. CERN/SPSC/76-13 ; SPSC/P78/Add 2,13 December 1977.
3. CERN/SPSC/76-17/P-10 Add 1, 19 February 1976.
4. F. Bleezacker *et al:* report UCSB TH-18, 1976.
5. W. Lee: *Proc. Int. Symp. Lepton and Photon Interactions at High Energies,* (Hamburg, 1977) p. 555.
6. B. Margolis: Phys. Rev. **D17** (1978) 1310.
7. CERN/EP/PHYS 72-25, 26 July 1978 and Beam Dump Gargamelle Collaboration: submitted to the Topical Conference on Neutrino Physics, Oxford, 2-7 July 1978.
8. N. Cabibbo *et al:* PAR-LPTHE 78/12, June 1978.

PROC. 19th INT. CONF. HIGH ENERGY PHYSICS
TOKYO, 1978

B 4 Photoproduction at the SPS-& *p\ K*KT%+TC* and a Search for Charmed Mesons

Presented by A. KEMP

Bonn, CERN, Ecole Polytechnique, Glasgow, Lancaster, Manchester, Orsay, Paris LPNHE, Rutherford, Sheffield Collaboration

This paper presents some of the first results from the Omega Tagged Photon Collaboration at the CERN SPS. The physics topics are:

1) $\gamma p \to \phi p$
2) $\gamma p \to \rho'(1500)p$
   $\quad \mapsto \pi^+\pi^-\pi^+\pi^-$
3) $\gamma p \to K^+K^-\pi^+\pi^-$
4) $\gamma p \to$ Charmed mesons

The experimental arrangement for these measurements is shown in Fig. 1.

The tagged photon beam was produced from an 80 GeV tertiary electron beam from the SPS. The photons were directed at a 670 mm liquid hydrogen target situated in the Omega magnetic field; the mean field was 0.9 tesla. Photoproduced particles were detected by spark chambers and wire proportional chambers inside the magnetic field region and by drift chambers at the downstream end of the magnet. A 32-cell Cerenkov counter, placed downstream of the drift chambers as shown in Fig. 1, was used to identify *K** and $p^\pm$, A large lead-glass array was used to detect f-rays; the results of measurements involving 7r°'s will be reported at a later date.

L Elastic <j> production

The trigger for process (1) required two or three charged prongs with the requirement that at least one track passed through the Cerenkov and was below the threshold which was 5 GeV/c for *x**, 17 GeV/c for *K** and 34 GeV/c for $p^\pm$. Consequently the data is restricted to the range 20 GeV<$£_r$<35 GeV. The /-distribution of events in the *§* peak is given by :

$$d\sigma/dt \cdot BR = ae^{bt}$$

with

$$a=(1.18\pm0.15)\ \text{nb GeV}^{-2}$$
$$b=(5.5\pm1.2)\ \text{GeV}^{-2}.$$

Thus *o-(rp-^0p)-BR(<p^K*$^+$*K-)=2l5±l3* nb (±24 nb systematic error)

The resulting value *o(yp-*<f)p)=442±29* nb agrees well with the results from the Santa Barbara-Toronto-Fermilab group.

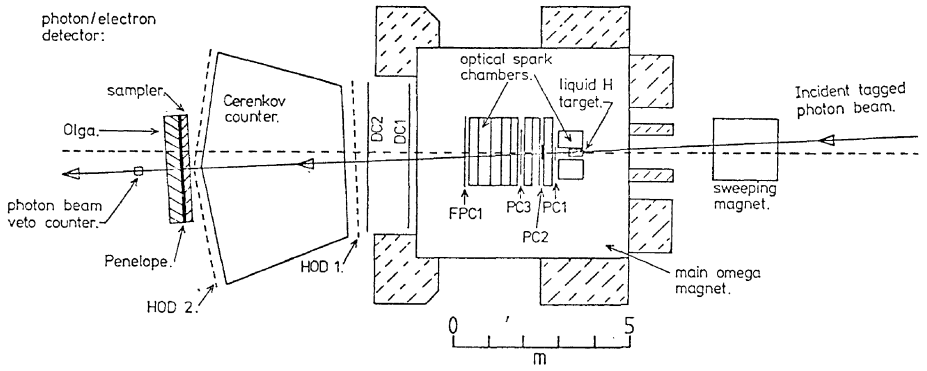

Fig. 1.

2. p\1500)

The trigger requirement was >4 particles leaving the target volume and reaching PC3 (Fig. 1). Reaction (2) was selected by the requirement that $|E_r - 2E_K| <$ GeV; where E_r and E_{tt} are the energies of the incoming photon and outgoing pions respectively.

The 47T invariant mass distribution is shown in Fig. 2. Production is peripheral (ae^{bt}) with a slope parameter è=5.1±0.2 GeV"^{2} for M(4TT)< 1.7 GeV. In contrast to peripheral phase space, which peaks at a mass ~3.5 GeV/c^2, the data show a broad enhancement centred at 1.5GeV/c^2, FWHM ~0.5GeV/c^2. We identify this with ^(IfSOO) $_{seen}$ by other authors. The $7t^+iz$~ mass distribution shows a strong ^(770) signal, ~1/2 *p* per event. There is no evidence for $p°p°$ decay, as expected if $C = -1$. A maximum likelihood fit shows that $J^p = l$~ decaying to pn^+iz~ dominates, as shown by Fig, 2.

5. *-fp-+K⁺K~7i:⁺7t~*

This channel is of interest since high mass vector mesons, in particular recurrences of the 0, are expected to decay into *K*K7z.* Events were selected to have topology compatible with channel (3), having two tracks identified as *K's* (momenta 5-17 GeV/c) by the Cerenkov counter, and by requiring that $|E_r - E_V| < 1.5$ GeV. We estimate a channel cross section of *15t\l* nb. From a study of events with a recoil proton we estimate the contamination from $pp7r^+7r$~ to be ~25%.

The K^+K~ TC^+n~~ mass distribution is shown in Fig. 3a. In contrast to the expectation from peripheral phase space (solid line), a broad threshold enhancement is present. The shaded histogram in Fig. 3a shows that there is a significant *K*Kiz* content whereas Fig. 3b shows no enhancement for $<p7z^+7i$~. There is no evidence for the decay *K*K*.* The momentum transfer distribution (not shown) is peripheral

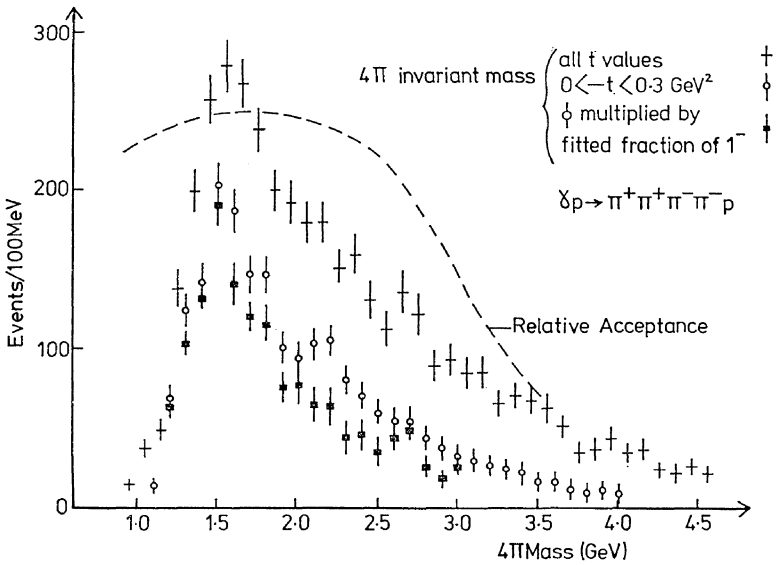

Fig. 2.

with a slope - 5 GeV"^{2} for *M{KKnn)<2* GeV/*c*\

In summary, the data show a peripherally produced threshold enhancement that decays to *KKTZTZ* and *K*KTT,* but not to *(pit-it.* We remark on the similarity to the *p'* seen in *yp-~>p-K*$^+$*K+7Z~7Z~.*

4. jp-> charmed mesons

The trigger requirement in this case was a multiplicity > 4 and at least one track > 5 GeV/*c* which did not fire the Cerenkov. Events for the present analysis were further selected off-line by a more precise test of the Cerenkov requirement. Data were also recorded which did not have to satisfy the Cerenkov requirement and these will be the subject of a separate analysis, including *K°* and *A*\ at a later date.

The acceptance for inclusive D-meson production was obtained from a Monte Carlo simulation which took into account the trigger requirements and off-line cuts. The acceptance is approximately 0.4 for all values of $x=pz/p_{Ltm\&}x$ greater than zero and for $p_T<$ 1.0GeV/c.

The mass resolution was estimated from simulated data and from fitting the #*(890) data in the *Kn* channels. The fits give a resolution at the *K** mass of 38 MeV (FWHM); this scales to 76 MeV at the *D* mass, assuming

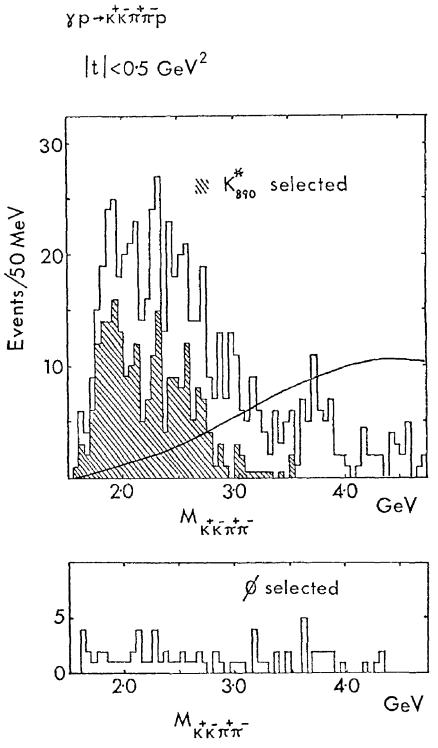

Fig. 3.

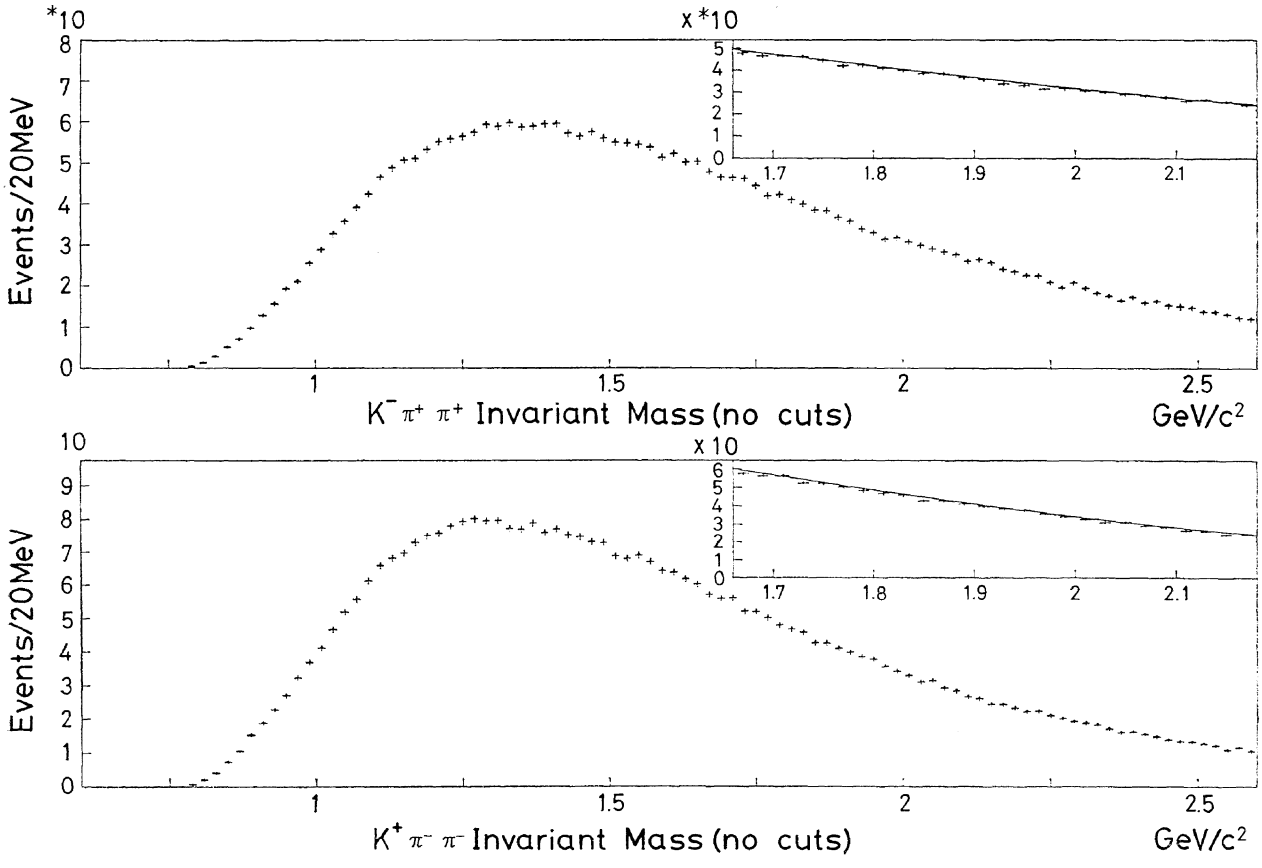

Fig. 4.

similar momentum distributions in each case. Similar values were obtained from the simulation. For the *KTZTC* channels we have taken *16* MeV FWHM.

Mass distributions for $K^{*''\wedge}$ and $K^{\wedge\wedge}n^{\wedge}$ show no significant peak at the mass of the *D.* We therefore deduce, for our sensitivity of 60 events/nb, limits on *a-B-e* at the 90 % confidence level *(e* is the product of acceptance and efficiency).

Using published values of the branching ratios we obtain upper limits on the inclusive cross sections for *D* production; these are given in Table I where we have taken the values of *a-B-e* and divided by *Be* without taking the errors on *B* and *e* into account. The limits range from 0.4 to 1.0 *jub.*

The interpretation of these data in terms of a total charm production cross-section is strongly model dependent, however since pair production of i)-mesons is included in either of the sums $D^{\circ}+D\sim$, or $D^{\circ}+D^{+}$ we see that the present limit is about 1.5 *jub* for the *x* range accepted.

In order to attempt to obtain a lower limit on associated production, we nave examined the spectra for $D\sim$ and D° decays in the case where the *D* has more than half of the incoming photon mementum. The resultant mass plots are shown in Fig. 4 and give the limits in Table II, thus the upper limit on associated production is about 0.8 *jub.*

Table I. Limits on σ_D.

Decay channel	Upper limit $\sigma \cdot B$	B	σ^*
$D^0 \to K^-\pi^+$	7 nb	$0.018 \pm .005$	0.4 μb
$\bar{D}^0 \to K^+\pi^-$	19 nb	$0.018 \pm .005$	1.0 μb
$D^+ \to K^-\pi^+\pi^+$	34 nb	0.039 ± 0.010	0.9 μb
$D^- \to K^+\pi^-\pi^-$	21 nb	0.039 ± 0.010	0.5 μb

Table II. Limits on σ_D for $p_D/E_\gamma > 0.5$ for $\bar{D}$ states

Decay Channel	Upper limit $\sigma \cdot B$	B	σ^*
$\bar{D}^0 \to K^+\pi^-$	10 nb	0.018 ± 0.005	0.5 μb
$D^- \to K^+\pi^-\pi^-$	10 nb	0.039 ± 0.010	0.3 μb

* Column 2 divided by column 3 with no allowance for error on *B.*

PROC. 19th INT. CONF. HIGH ENERGY PHYSICS
TOKYO, 1978

B 4 Hadronic Content of Photons

Presented by D. O. CALDWELL

University of California, Santa Barbara

Using the tagged photon beam we developed at Fermilab, our group has performed three experiments which display the hadronic content of high energy photons. These are measurements of (1) the total photon cross section on hydrogen, to see if there is a rise with energy ^ as is displayed by hadrons ; (2) the total photon cross section on nuclei to see from "shadowing" effects the strong interaction of photons; (3) the photoproduction of vector mesons, to compare with 7r-p and K-p cross sections, via vector-meson-dominance (VMD) and the quark model.

The measurements are difficult because the electromagnetic background is hundreds or even thousands of times larger than the hadronic signal. There is not time to discuss experimental details, but the essential idea is to veto electromagnetic events at small angles (using the equality of the incident photon energy and the downstream electromagnetic energy) and to detect hadrons at larger angles. To avoid missing hadronic events, hadron detectors covered at least 90° in the *y-p* center of mass system. The longitudinal spacing of the detector system, which

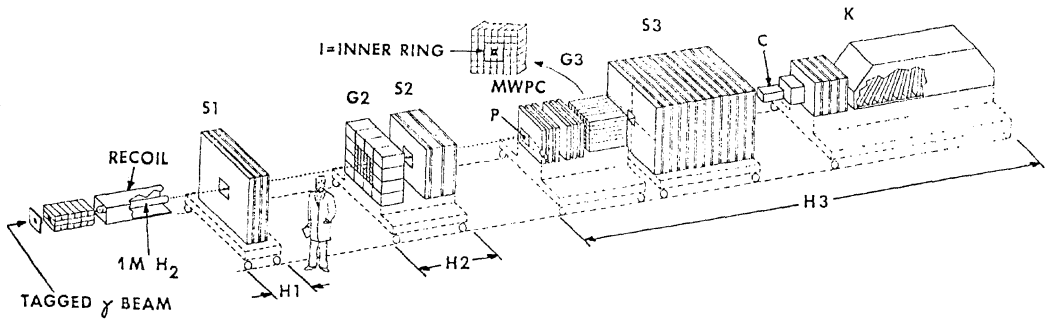

Fig. 1. The detector system. The longitudinal spacing was varied with the incident electron energy.

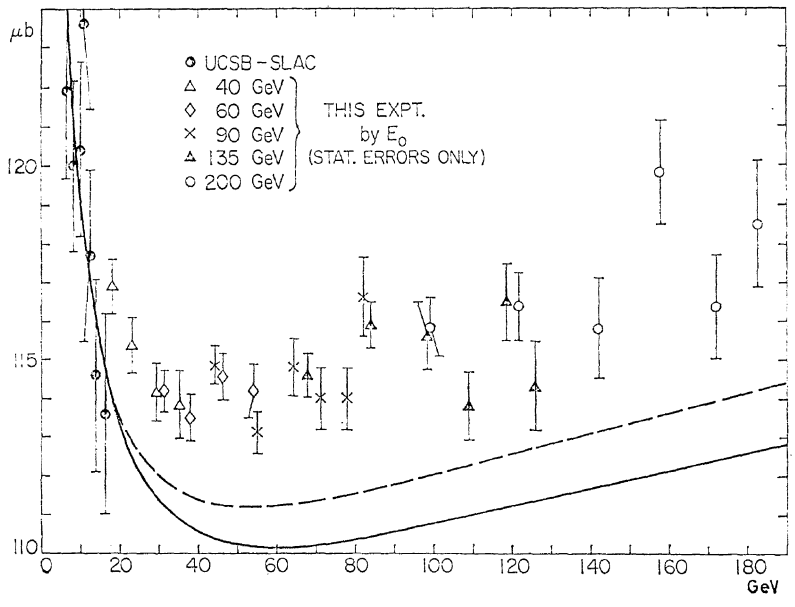

Fig. 2. The total photon cross section on hydrogen as a function of the photon energy.

is shown in Fig. 1, was varied when the incident electron energy was changed. Energies of 40, 60, 90, 135, and 200 GeV were used, from which photons of 45 % to 93 % of the electron energy were tagged. Thus there was considerable overlap of *y* energy for each electron energy, and as a further check some data were taken at 60 GeV with the 90 GeV geometry. The small double bremsstrahlung corrections were checked by employing different radiator thickness.

The results of the hydrogen cross section are shown in Fig. 2, where the rise in the cross section is clearly seen in this plot with a highly suppressed zero. The lower energy points join on to the earlier UCSB data from SLAC in the falling region of the curve, there is a broad minimum around 40 GeV, and then a rise of about 4/*b up to 185 GeV. The shape of the curve is consistent with hadronic cross sections, as checked by using *a, p+<o+ <j>* vector dominance model and obtaining the vector meson cross sections using the quark model and measured 7r-p and K-p total cross sections. The solid curve (using coupling constants from A-dependent vector meson photoprocuction) and the dashed curve (using the çS coupling constant from colliding beam data) lie below the data, probably because of a 2 to 6 */Ltb* contribution from charm-anti-charm states.

For the total cross section data for carbon, copper, and lead, we had to make especially careful checks that no hadronic events were missed, since there is a tendency in heavy nuclei for hadrons to be produced at wider angles. A full energy dependence was obtained for copper (20 to 185 GeV), while the A-dependence was measured over a more limited energy range (45 to 82 GeV). It will be noted that the copper cross section (Fig. 3) shows no rise at high energy, as is typical of hadron-nucleus cross sections. Thus if one looks at the shadowing, by plotting the ratio

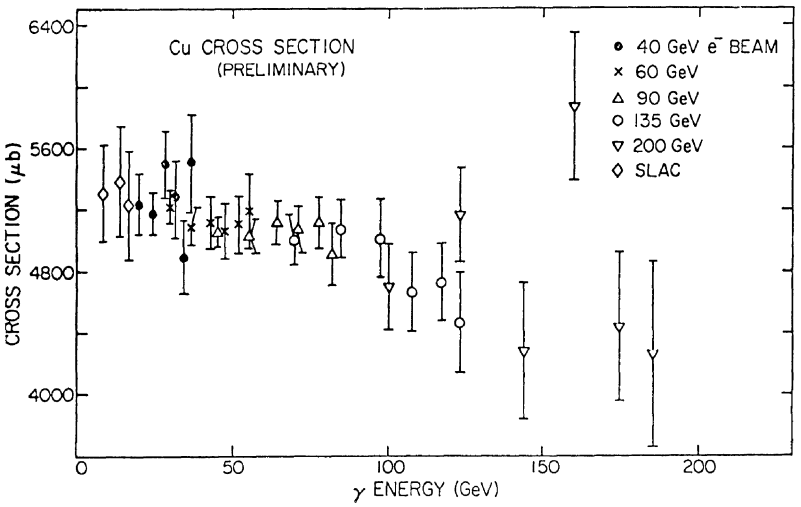

Fig. 3. The total photon cross section on copper as a function of the photon energy.

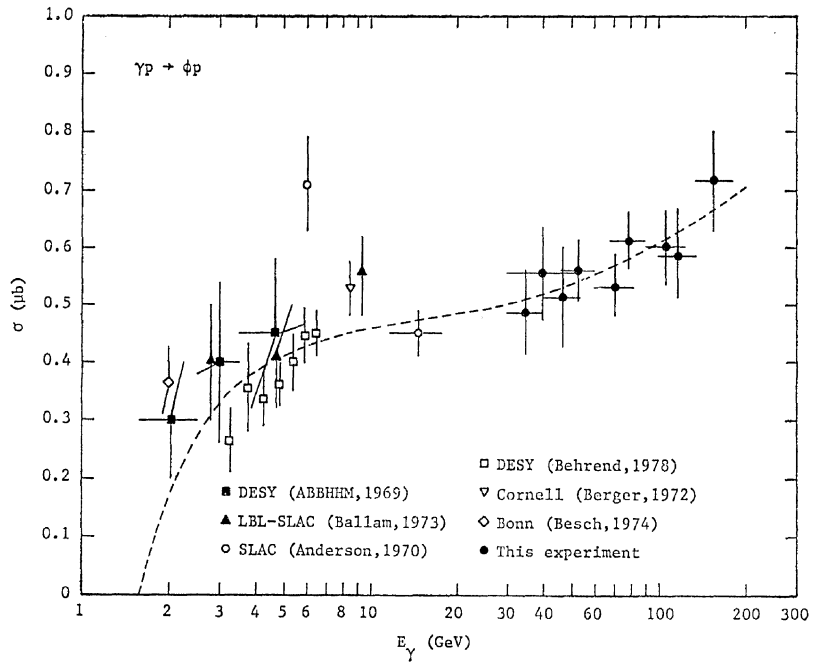

Fig. 4. § photoproduction cross section.

of the nucleus cross section to that for the constituent nucléons, then the rise in the nucléon cross section gives a decrease in the ratio, corresponding to an increase of shadowing with energy. The increase with energy can be attributed to the rise in the vector meson cross sections, as well as to some contribution from higher mass states which at the higher energies can exist longer and hence have more chance of interacting with the nucleus.

There is insufficient time to explain how vector meson photoproduction could be measured in this total cross section experiment, but suffice it to say that for events in which only two charged tracks were observed (no 7T^{0}s), *p* and <*p* decays were clearly and cleanly separated by the angular separation of the tracks. The *p* cross section results agree very well both with other data and with the combination of vector meson dominance and the quark model, employing measured 7r$^{\pm}$-p cross sections.

For the more difficult <*f*> measurement, it is worth plotting the § mass peak in terms of the track separation, normalized by the maximum separation expected for a ^ of the incident *j* energy. An assumption of an isotropic decay does not fit the data, while that of ^-channel helicity conservation does indeed fit. This is to be expected if the ç▷s were diffractively produced. The <*fi* cross section

is shown in Fig. 4 along with lower energy data. There is a striking rise of the cross section by almost a factor of two over the energy range of 35 to 185 GeV. However, if the fit to these data (dashed line) is compared with the vector meson dominance and the quark model, using $K^{\pm}$-p and *rc~-p* elastic cross sections, then this rise is just what is expected. Once again the hadronic nature of the photon is displayed.

PROC. 19th INT. CONF. HIGH ENERGY PHYSICS
TOKYO, 1978

B 4 Muon Scattering at Fermilab

Presented by R. WILSON

Chicago-Harvard-lllinois-Oxford Collaboration

In this paper we report the preliminary results of the analysis of hadron production in deep inelastic scattering at 219 GeV, using the Fermilab muon beam and the Chicago Cyclotron spectrometer. The results are compared with the analysis of a 150 GeV muon beam presented at the Tblisi meeting[1], in Physical Review Letters[2] and in a forthcoming paper in Physical Review.[3]

Our results on the structure function $F_{\%}\{x)= \nu W_2$ have only slightly changed since the Hamburg meeting[1] but we can now derive $R = <j_L/a_T$ by comparing data at 3 energies. The result, averaged over all of our data, is 0.52^0.25, with most of the error systematic. The QCD prediction is smaller, and if we fit to $4(kt)/Q^2$ we find a better fit than $R=$ const, with </c|>~0.3, $V</t^2_r>$~0.55 GeV.

We have also extended our data to low Q^2 and for i?=0.5, we find $<r_r$ = 115 *fcb* in agreement with the total cross section of 117 *fib* (Contribution No. 647).

Unless otherwise specified, the data are presented with the following kinematical cuts $q^2>l$, 50<^<200, $p^2_T<3$, 0.2<z<0.9.

The hadrons, to be observed, must pass through the cyclotron magnet, and this gives a cut of z>0.1, varying somewhat with *s*. To make this a cleaner cut than the apparatus acceptance would give, we have looked only at high *s* and z>0.2.

2 Dependence

We present in Fig. 1 the invariant structure

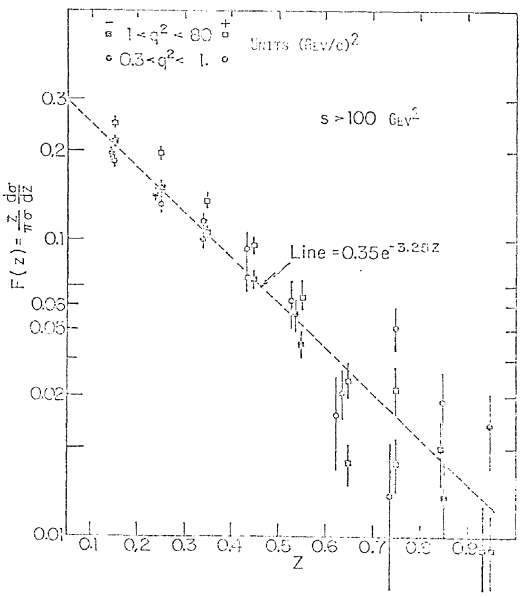

Fig. 1. *F(z)* for $q^2>\backslash$, $03<q^2<l$ and $s>100$.

function

$$F(z)=\int_0^{2\pi}\int_0^{p_T^2} \frac{E}{\sigma}\frac{d^3\sigma}{dp^3}\,dp_T^2\,\frac{d\phi}{2\pi} = \frac{z}{\pi\sigma}\frac{d\sigma}{dz}$$

for all charged hadrons. For comparison the line is F(z)=0.35 e"^{3}-^{25}*, which was used by us previously.[2,3] The agreement is a good illustration of Feynman scaling.

In Fig. 2 we present the +/— ratio as a function of $a)=l/x=2Mv/Q^2$. The line is the prediction of Dakin and Feldman[4] which follows from the quark model; at low *OJ* the hadrons are along the quark direction and tend to take the charge (positive) of the struck quark. At high co_9 the hadrons come from the photon disassociation and the photon

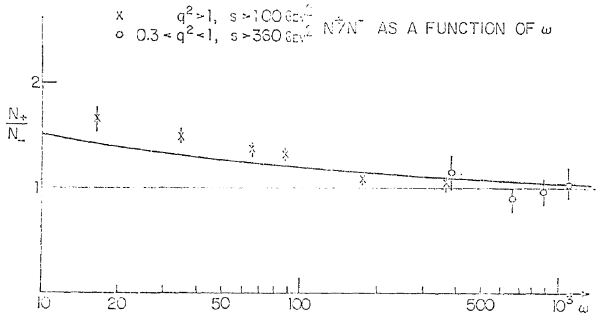

Fig. 2. N^+/N as a function of *co* where $q^2>l$, $s>$ 100, $0.3<\#^2<1$ and ^> 360.

has no net charge. This is also true of the +/— ratio as a function of z.

In order to go into more detail of variations of F with Q^2, we studied Q^2 dependence of the moments of z, e.g. <V>, $<z^2>$, $<z^3>$, and found no obvious variation.

p_T Dependence

The momentum of the hadrons transverse to the virtual photon direction is particularly interesting. This can be described by a sum of 3 terms.

$$\langle p_T^2\rangle=\langle p_T^2\rangle_{\mathrm{QCD}}+\langle k_T^2\rangle+\langle k_D^2\rangle \qquad (2)$$

The first of these terms comes from corrections of order (Q^2) to the simple quark model. The second and third are more *ad hoc;* k_T is the *transverse* momentum of the produced quark in the laboratory frame (because the quark is confined, the uncertainty principle tells us that it must have a transverse momentum) and k_D is the transverse momentum of *dressing* the quark to become a hadron, and both k_T and k_D may have z dependence.

The QCD term has been calculated for us by Mendez.[5] To the extent that the model applies generally, k_D should be the same for e^+e^- scattering. A comparison of the data at comparable values of x'^z and x_{fl} shows that the main dependence *on* p_T seems to be the same for the two reactions as shown in Fig. 3. The e^+e^- data[6] *also* shows the seagull effect suggesting that $(k^2_T\}=0$. Although the e^+e^- data does not extend above $x_{„}>0.4$, $(p_T y$ for ^{our} experiment does not *rise* for $x'>0A$ so that there seems no room for the $(k\%y$ term unless $(k^2_D y$ falls with x_{fl} above $x=0A$. This clearly needs further study.

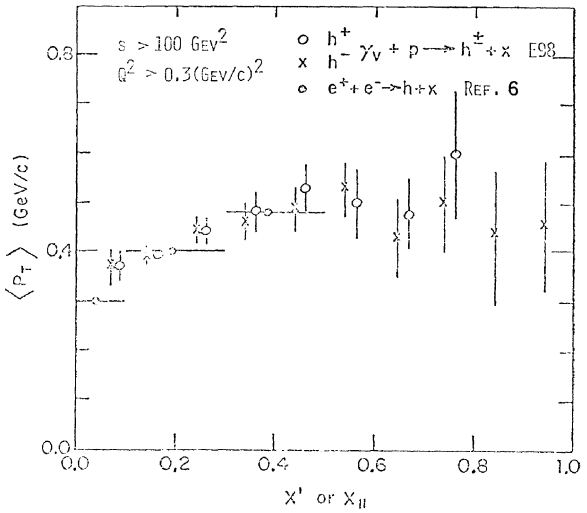

Fig. 3. $(p_T y$ vs x' or *n for ^+p-^h±+x or e^+e~-> h+x.

Angular Correlations

We can look for angular correlations by measuring the average value of {cos <*f)* and $<\cos^2 <f)$ where <*f*> is the angle between the hadron and the leptonic plane in the plane perpendicular to the virtual photon.

One feature about Mendez' calculation[5] is that <cos 20} is always positive. The contribution <(cos 0) from quarks dressing into hadrons is positive. That from gluons dressing into hadrons is negative. Two curves are provided; one where the gluons *do not* dress into hadrons (D^=0) and the other where they dress as much as quarks $(D_g=D_q)$. It is clear that the predicted effects are greater than our data shown in Fig. 4. Another interesting angular correlation is with the recoil proton. The same arguments that suggest that the hadrons at high z represent the dressing of the struck quark, suggest that the *recoil* also contains this inforamtion.

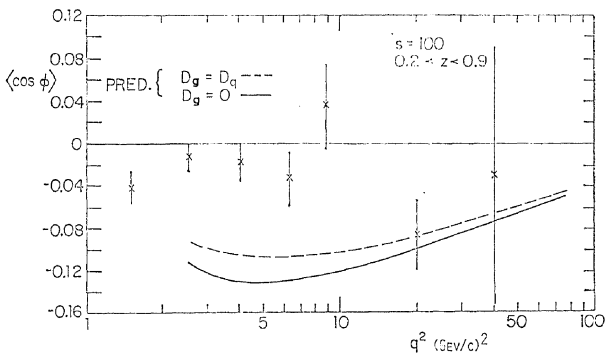

Fig, 4. <cos 0> as a function of q^2 for $0.2<z<0$-9 and $_t y>100$ with QCD predictions of Mendez.

{cos <*j*>) for these recoil protons vs z_H for the accompanying fast hadron also shows no effect.[7] It is clear that "clean tests of QCD"[8] do not work; presumably we can wriggle out of them by the non-perturbative effects of the initial momenta.

The recoil proton momentum (energy) is, in itself, interesting. It follows exp (—7.6t). This is a steeper fall off than seen at lower energies.[9]

Kaons

Over a limited kinematic region we have measured charged *k* mesons and protons by using a threshold Cerenkov counter following the C.C.M. (thesis of J. Proudfoot).

At high momenta, *%* and *k* count in the Cerenkov counter and p* do not. We can then see a small p* signal. At lower momenta, *k** also fail to count and we find a singal sufficiently large that we attribute it almost entirely to *k** mesons.[10]

The *kjn* ratio rises to about 1/2 as a function of *z* and *k** mesons have a higher *p* and z than TT* mesons. The *kjit* ratio as z-+l is consistent with 1/2 as suggested by Feynman, Field and Fox.[11]

At the larger *z* where the leading quark counts, *($_T$}k>(pT%* suggesting that eigher *(k_T)* or *(k_Dy* is greater for kaons than for pions in agreement with the spread due *to* the necessary gluon bremsstrahlung.

Vector Mesons

By examining the downstream hadrons, we have looked at the elastic vector meson production[10] on a small data sample

$$\mu + p \rightarrow V^0 + p$$

The Q^2 dependence fits the well known Vector Dominance behavior for a propagator *(M^2/(Q^2+M$)y* contrary to Soding's comment (Thesis of L. Myrianthopoulos) and that the <2^2-»0 cross section follows the Vector Dominance prediction. We also have preliminary data on *$* mesons. The problem here is that the low energy *k* mesons have a small opening angle and an electron-positron pair could be misidentified as a <P°. We avoid these by a transverse momentum cut.

The ratio $[\sigma_\phi/\sigma_\rho]_{Q^2\to 0}$ $= 0.66 \pm 0.02$, $\nu = 120$
$= 0.08 \pm 0.02$, $\nu = 70$.

The *t* distributions are for exp $(-bt)$,

b_ρ	120 GeV	7.7 ± 0.5	70 GeV	6.9 ± 0.5
b_ϕ	120 GeV	5.3 ± 1	70 GeV	4.2 ± 1

References

1. A. L. Sessoms *et al:* "Hadrons Produced in Deep Inelastic Muon Scattering at High Energies," presented at the 18th International Conference on High Energy Physics, Tblisi, July 1976.
2. W. A. Loomis *et al*: Phys. Rev. Letters 35 (1975) 1483; H. L. Anderson *et al:* Phys. Rev. Letters 36 (1976) 1422.
3. W. A. Looomis *et al:* "Hadron Production in Muon-Proton and Muon Deuteron Collisions," in press.
4. J. T. Dakin and G. J. Feldman: Phys. Rev. 8D (1973) 2862.
5. A. Mendez.: "QCD Predictions for Semi-Inclusive and Inclusive Leptoproduction," Preprint, Dept. of Theoretical Physics, Oxford 28/78.
6. G. C. Hanson: "Jets in e^+e" Annihilation," SLAC-PUB-2118, May 1978.
7. This was shown by A. L. Sessoms at the Orbis Scientac, University of Miami, Coral Gables, FL, January 1978.
8. H. Georgi and D. Politzer: "Clean Tests of QCD in jup Scattering," Phys. Rev. Letters 40 (1978) 3.
9. Ahrens *et al:* Phys. Rev. D9 (1974) 1894; Work reported at APS Meeting, May 1977.
10. W. R. Francis *et al*: "Diffractive Production of Rho Mesons by 147 GeV Muons," Phys. Rev. Letters 38 (1977) 633.
11. R. P. Feynman, R. D. Field and G. C. Fox, Nuc. Phys. B128 (1977) 1.

PROC. 19th INT. CONF. HIGH ENERGY PHYSICS
TOKYO, 1978

B 4 Deep Inelastic Muon Scattering at 270 GeV at Fermilab

Presented by K. W. CHEN

Michigan State University, East Lansing, Michigan 48824

The nucléon structure function, $i>W_{2r}$ has been measured up to $q^2 = 150$ (GeV/c)^2 and up to $W=21$ GeV. The data exhibit a threshold-like pattern of scaling violation. Compared with lower energy data the present results show a rise in ${}_{V}W_2$ with q^2 at low and moderate x. This rise in νW_2 is consistent with a threshold-like behavior in the variable W.

Recent experiments[1~3] on deep inelastic muon and electron scattering have established significant deviations from Bjorken scaling[4] up to $\wedge^2$ = 50 (GeV/c)^2. The nucléon structure function, νW_2, can no longer be expressed as a function of a single scaling variable, $x=q^2/2M\nu$.

The present experiment, carried out at Fermilab, increases significantly the kinematical range thus far explored. This is mainly the result of the high incident muon energy of 270 GeV, almost double that of previous studies.[1,2] For a total of $3\text{x}10^{10}$ incident muons 0^+ and *(JT)*, 10^6 deep inelastic events above q^2=5 (GeV/c)^2 are recorded. The target consists of 7.4 m long (4,260 g/cm^2) iron-scintillator calorimeter which also measures the final state hadron energy. Following the target is a 745 g/cm^3 thick steel hadron shield and a spectrometer consisting of eight fully powered toroidal magnets (4,973 g/cm^2 thick and about 90 cm in radius). Both the hadron shield and spectrometer are interleaved with wire spark chambers. In addition, three vertical and horizontal trigger banks of scintillation counters are positioned within the spectrometer. These must be penetrated by the scattered muon for the event to be recorded. A set of three scintillation counters (15.9 cm radius) centered on the beam axis and placed in the back section of the spectrometer forms a veto which eliminates events with a penetrating particle at a small angle. A set of proportional chambers and beam halo veto (scintillation) counters define the incident muon. Figure 1 shows curves of equal apparatus acceptance in the q^2-ν plane. It can be seen that the acceptance is a smooth function of q^2 and ν. It exceeds 50% for all data reported here. In this Letter, only analysis of the JU^+ sample is reported.

The momentum of the scattered muon is determined from fitting its trajectory through the magnetic spectrometer. The fitting algorithm is based on detailed magnetic field maps, measured muon dE/dx values as well as calibration of the spectrometer with the muon beam and study of the high energy end of the scattered muon spectrum. Track finding efficiencies vary from 80% at low q^2 to 99 % at high q^2. The resolution of the spectrometer is known to be about 10%, while the central value is calibrated to about 0.7%. The scattering angle is known to 0.4 mrad. The energy of the incident muon is determined to within 0.75% by several independent methods.

The values of the structure function, νW_2 per nucléon are obtained by comparison of

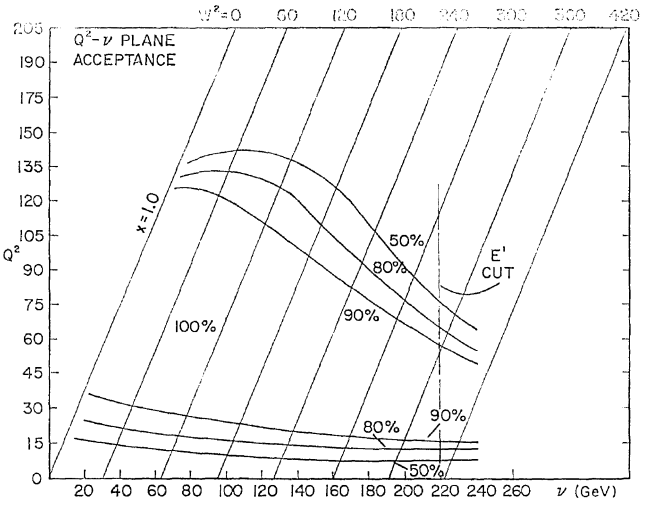

Fig. 1. Contour plot of apparatus acceptance as a function of q^2 and ν. Also shown are lines of constant W^2 which are labelled at the top of the figure. The E' cut requires the scattered muon to have total energy larger than 50 GeV.

data with a Monte Carlo simulation based on fits[5] to νW_1 and νW_2^D. The simulation includes effects of Fermi motion of the nucléons in the iron nucleus, radiative corrections and wide angle bremsstrahlung in simulating deep inelastic scattering. Further analysis treats data and Monte Carlo events identically. The data presented below show only statistical error and do not include the 10% systematic and normalization uncertainties.

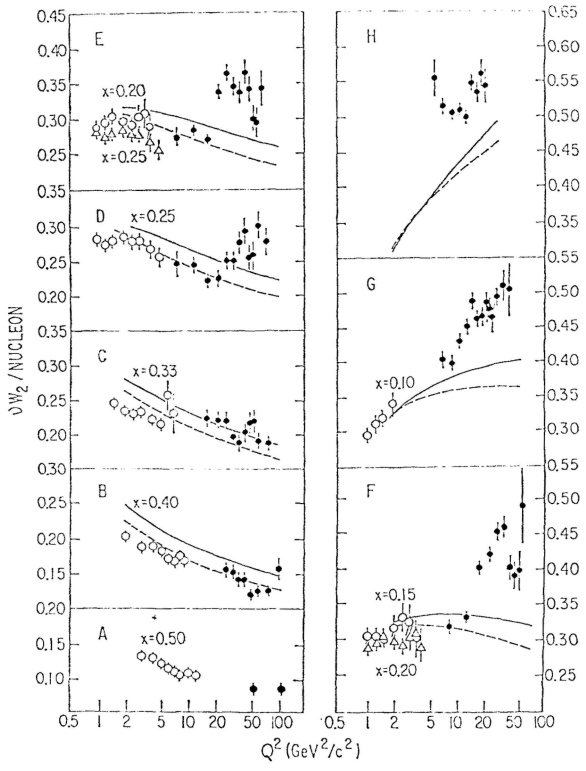

Fig. 2. Nucléon structure function, νW_2, as a function of q^2, for successive regions in *co:* (A) $co=2_9$ (B) 2<o><3, (C) $3<\text{æ}<4_9$ (D) $4<o)<5$, (E) $5<co<7$, (F) 7<a><10, (G) $10<o)<16$, (H) 16<o><38. The open circles are data from ref. 3. Present data agree reasonably well with the trend established in earlier studies at low and moderate q^2 but show a marked increase of the structure function at high q^2. Vertical bars indicate statistical errors only.

The deviations from scaling can be seen clearly in Fig. 2 (A-H) where νW_2 is plotted versus q^2 for successive regions in x. For <^x)=0.5, νW_2 falls with q^2 continuing the trend of lower energy data[6]. At lower values of <x> the present data also join the initial downward trend established earlier[1,2] at moderate q^2. However, the graphs show a reversal of this trend in the newly explored high q^2 regime. The behavior of $\nu W_{\%}$ versus q^2 for the various values of x is consistent with that expected from a threshold behavior in the variable W^2.

This observed threshold-like behavior cannot be explained by any known systematic effects such as uncertainties in measurement of E_0, E' and 6 or in the application of radiative corrections and corrections for wide-angle bremsstrahlung and Fermi motion.

It is a pleasure to acknowledge staff of Fermilab for their support. We thank K. Thorne for his help in data reduction.

This research was supported in part by the National Science Foundation under Grant No. 60950 and by the Department of Energy under Contract No. E(ll-1)-1964.

References

1. C. Chang *et al:* Phys. Rev. Letters 35 (1975) 901.
2. H. L. Anderson *et al :* Phys. Rev. Letters 38 (1976) 1450.
3. E. M. Riordan *et al* : SLAC Report No. SLAC-PUB-1634, 1975 (unpublished).
4. J. D. Bjorken: Phys. Rev. **179** (1969) 1547.
5. S. Stein *et al:* Phys. Rev. **D12** (1975) 1884.
6. Only the data of ref. 3 for $(\nu W_2^D/2)$ are shown for comparison. The muon proton deep inelastic scatterng data of ref. 2 refer to the structure function of the proton only and are not plotted.

PROC. 19th INT. CONF. HIGH ENERGY PHYSICS
TOKYO, 1978

B 4 The Electromagnetic Size of the Neutral Kaon

Presented by B. WINSTEIN

The University of Chicago

It is easy to see that SU_3 symmetry breaking can lead to a K° charge structure. In the framework of the quark model, the heavier s quark will be confined to smaller radii thus giving the K° a positively charged core. As a result, electrons will be attracted to ^°'s (and repelled from $R^{\circ 9}s$), but only when the electron is "inside" the kaon. The charge radius of the K\ defined by <U^a>=IV?, should then be negative. Quantitatively, one expects $(R^2(K^0))$ ^—0.06fm^2 where the magnitude depends on the *difference* between the strange and non-strange quark masses.

Feinberg[1] first pointed out that the K° could have a charge structure, and Zel'dovich[2] as well suggested the method of measurement on which this work is based: the detection of the interference between coherent regeneration from the nuclei and that from the atomic electrons of a target.

If we let/[6] be the K°~ e scattering amplitude, then the K°—e amplitude is given by f^e=—f^e. Thus, since f^e4=-f\ electrons will regenerate K_s from K_L.

In the exact forward direction, the atom (as well as the entire target) will coherently regenerate so that the rate is given by

$$R(0) \propto |f^N_{21}/k + Z f^e_{21}/k|^2$$
$$\simeq |f^N_{21}/k|^2[1 + 2Z\,\mathrm{Re}\, f^e_{21}/f^N_{21}]$$

and contains the interference term. Here f^N/k denotes the the nuclear regeneration amplitude whose modulus falls[3] with momentum, and /£[/&=constant= — $a/3$ <i?^{2}> is the electron regeneration amplitude where the last expression results from the expansion of the K° form factor; k is the kaon wave number.

At finite q^2, the rate (ideally) is given by:

Thus a comparison of the rate at $q^2=0$ with

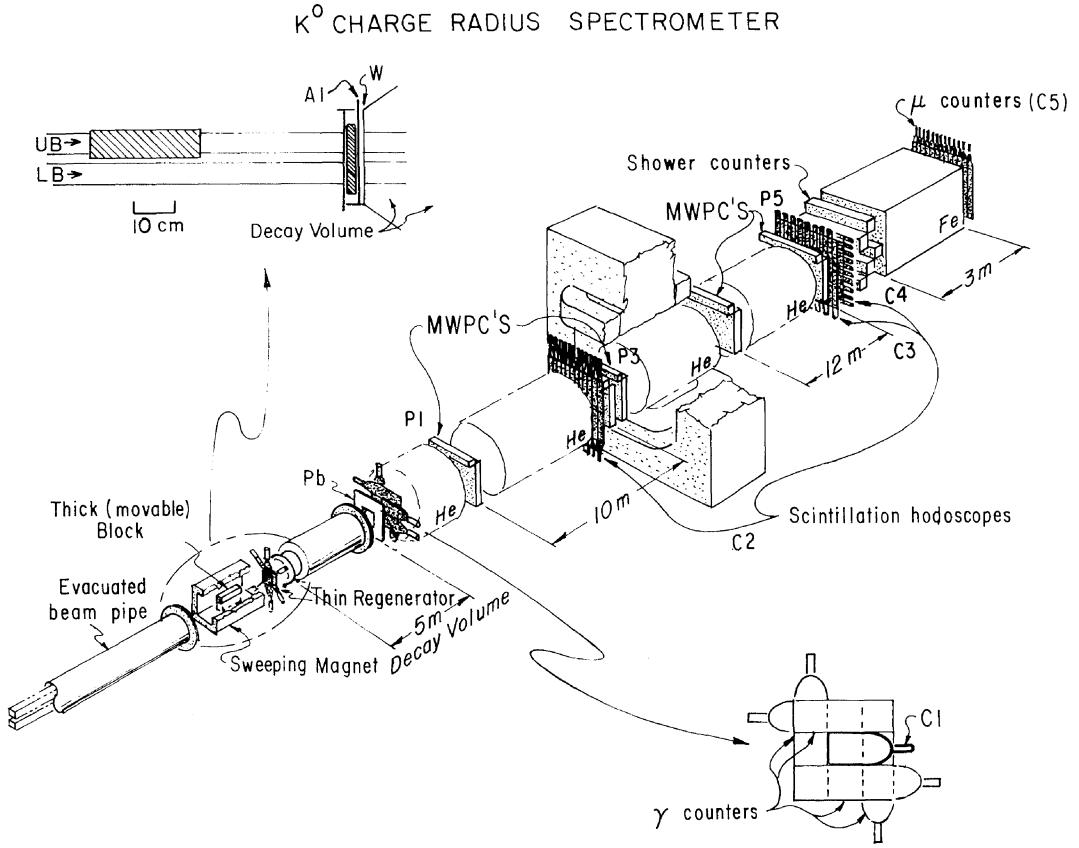

Fig. 1.

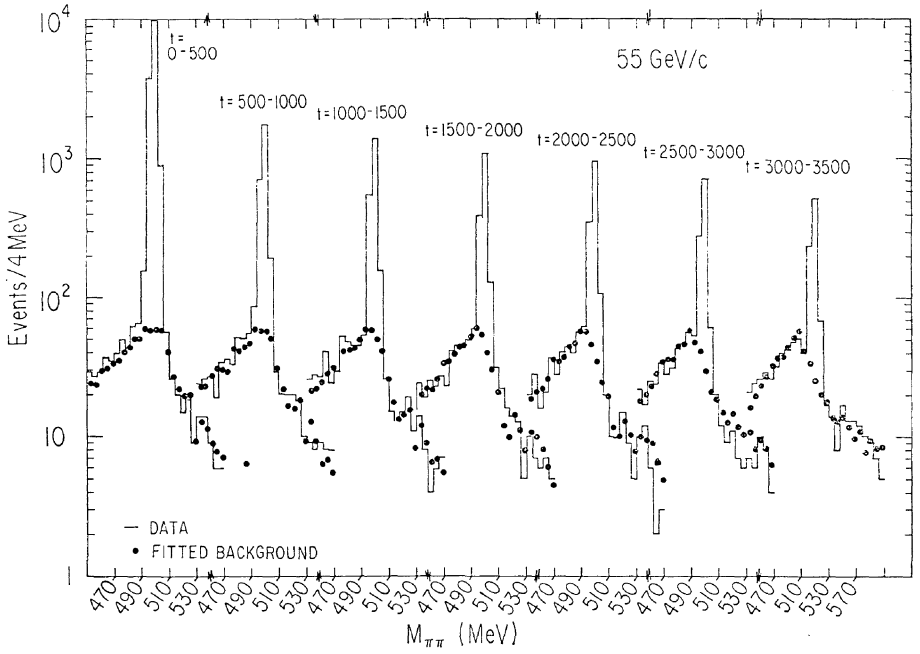

Fig. 2.

that extrapolated to $q^2=0$ from a high Z regenerator can reveal the contribution from the atomic electrons which then grows with momentum (about 3 % at 65 GeV/c. for Lead).

For the present work, we measured the two rates *independently* with appropriately optimized Lead regenerators for each. The difference in attenuation between the two regenerators was corrected for by a precise measurement[4] of the total cross-section. This feature minimized corrections for *CP* non-conservation and multiple scattering.

The measurements were performed *simultaneously* with the construction of a "double neutral beam" at Fermilab to eliminate normalization uncertainties. Coherent $(q^2=0)$ regeneration was measured in one beam with a thick regenerator while diffraction $(q^2>0)$ regeneration was measured simultaneously in the other with a thin regenerator.

Figure 1 shows the spectrometer. Each of the beams (1.5 cm separation) was 6 cmx 6 cm and contained about $3x10^5$ Z^'s/pulse from 30 to 100 GeV/c. The thin regenerator (covering both beams) was 2-cm (Lead) completely surrounded by anti-counters; the thick one was a 26-cm block positioned inside a sweeping magnet plus the thin one. The block was alternated between the beams every pulse ($2x10^5$ times) thus exchanging the roles of the beams. A restricted two-particle trigger initiated the MWPC readout.

The $35x10^6$ reconstructed events were further cut to isolate $\sim 2x10^6$ K^Q-^n+7t~ decays. To perform the extrapolation to <?^{2}=0, the small background from K_L->*Tiev* or *TT/UV* (normally rejected with shower counters and a muon filter) which "sneek in" to the *n-n* signal had to be understood and subtracted. Figure 2 shows the mass distributions in different q^2 regions for one momentum bin; the structure of the background is well represented by the use of the large sample of identified semi-leptonic decays.

Figure 3 then shows one set of extracted q^2 distributions. To extract the $q^2=0$ intercept of the elastic thin regenerator events, we must

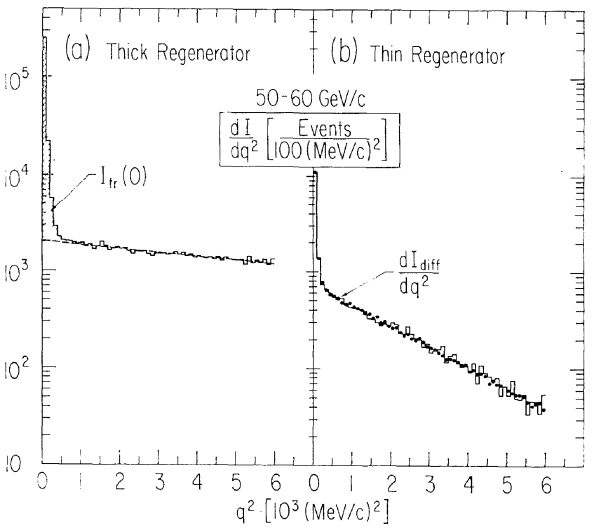

Fig. 3.

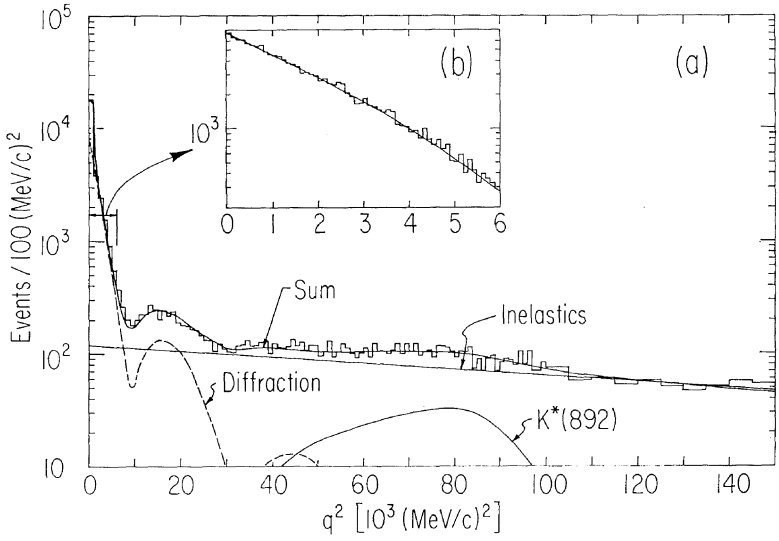

Fig. 4.

study the q^2 distribution at larger values than shown in Fig. 3.

Figure 4 displays the results of this study: the ^-distribution for all thin regenerator events together with a theoretical fit. There are four ingredients to this fit:

1) a coherent shape determined from thick regenerator events (see Fig. 3),
2) a diffracted shape (including multiple scattering) taken from an optical model,
3) Primakoff produced *K** (892) events with a decay to K_s n^Q and an unvetoed *TT*
4) an exponential distribution of inelastics.

We note that the clear observation of the diffraction minima filled in by the inelastics gives us confidence that the contribution of the latter near $q^2=0$ is correctly determined. The importance of using a Bessel-like function rather than an exponential for extrapolation is evident. Finally, a sub-class of the *K*(892)* events are directly detected when one or both of the *y* rays hit our shower counters. The q^2 distribution for these (j?$_r$>10 GeV) shows

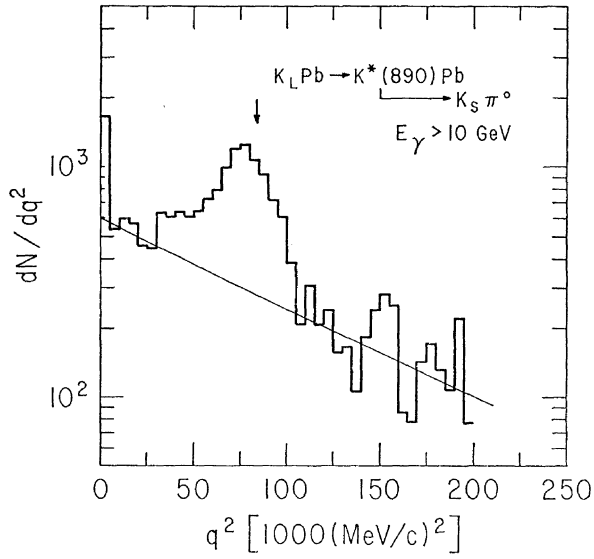

Fig. 5.

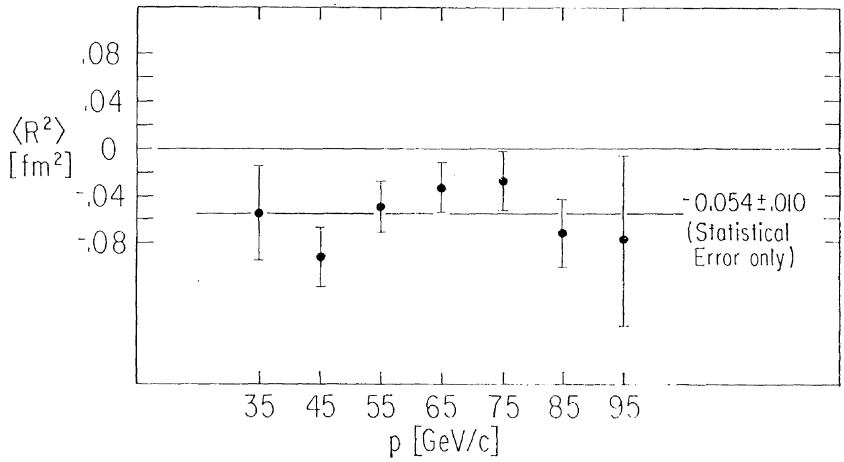

Fig. 6.

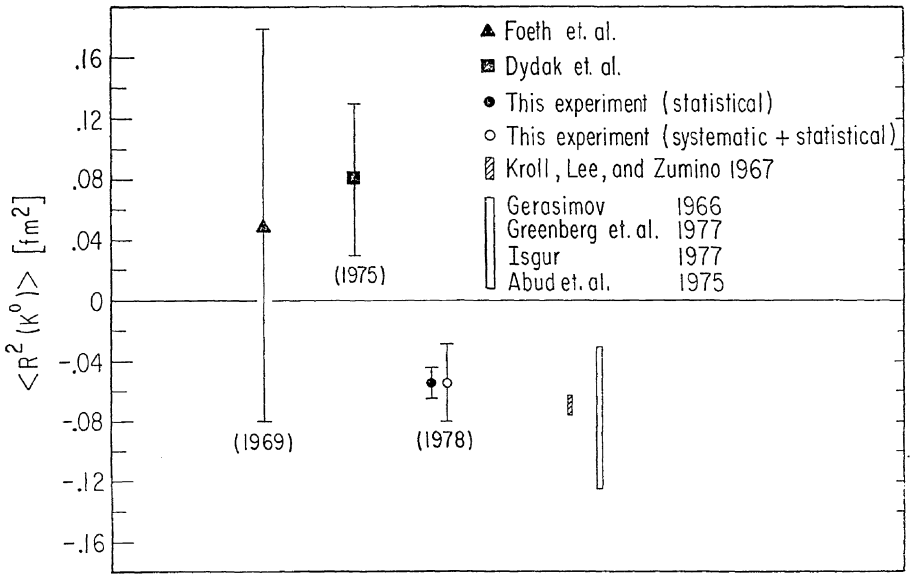

Fig. 7.

(a) From ref. 4 and additional data: a_T assumed constant for $50<p<100$ GeV/c.
(b) Parameter varied is rms nuclear radius.
(c) Re(/$_2$2)/Ini(/22)—0.010; error indicated is for change by ^0.005.
* Quoted errors are in many cases correlated.

the characteristic Jacobian peak (see Fig. 5).

The phase of the amplitude is measured using runs with the thin regenerator removed ($0 = -122^\circ \pm 1.8^\circ$), corrections for CP violation made, and the charge radius is then extracted in each momentum bin. Figure 6 shows the results with a_T, $\langle f \rangle$, and the extrapolation parameter held at their best values. The result is constant and negative «i?^{2}> = —.054 ±.010 fm^2) as predicted. With the inclusion of all systematic uncertainties (see Table) we obtain <i?^{2}>=-(0.054±0.026) fm^2. Fig. 7 compares our result with previous experiments[5,6] and recent theory[7] with which we are in good agreement. In particular our result rules out with 98% probability the positive sign in ref. 6.

References

1. G. Feinberg: Phys. Rev. **109** (1958) 1381.
2. Ya B. Zeldovich: Sov. Phys. JETP 9 (1959) 984.
3. A. Gsponer et al.: "Precise Coherent K_s Regeneration Amplitudes for C, Al, Cu, Sn, and Pb Nuclei from 20-440 GeV/c and Their Interpretation," paper number 1128, this Conference, and to be published.
4. A. Gsponer *et al:* "i^-Nucleus Total Cross Sections Between 30 and 150 GeV: Quantitative Evidence for Inelastic Screening," paper number 1132, this Conference, and to be published.
5. H. Foeth *et al:* Phys. Letters **30B** (1969) 276.
6. F. Dydak *et al:* Nucl. Phys. **B102** (1976) 253.
7. N. M. Kroll, T. D. Lee and B. Zumino: Phys. Rev. **157** (1967) 1376; O. W. Greenberg, S. Nussinov and J. Sucher: Phys. Letters **70B** (1977) 464; S. B. Gerasimov: Sov. Phys. JETP **23** (1966) 1040; M. Abud, R. Lacaze and C. A. Savoy: Nucl Phys. **B98** (1975) 215; N. Isgur, Acta Physica Polonica **B8** (1977) 1081 and Phys. Rev. **D17** (1978) 369.

PROC. 19th INT. CONF. HIGH ENERGY PHYSICS
TOKYO, 1978

B 4 Direct Determination of the Kaon Form Factor

Presented by E. TSYGANOY

Joint Institute for Nuclear Research

Determination of the kaon form factor in a space-like region has until now eluded experimental measurement. In electron-positron annihilation experiments the two-kaon final state is not dominated by simple resonance production and the extraction of the kaon form factor is not a straightforward matter, in contrast to the pion with its rho resonance dominance. For similar reasons electroproduction experiments cannot be usefully interpreted to produce the kaon form factor. Direct determination of a kaon charge radius by kaon scattering from electrons that had not been possible before Fermilab energies became available because the unique kinematic characteristics of scattering with a relatively massive projectile require such energies to produce momentum transfers sensitive to the kaon form factor.

We have used a 250 GeV negative kaon beam at the Fermi National Accelerator Laboratory to measure the cross section for elastic scattering from atomic electrons of a 51 cm long liquid hydrogen target for momentum transfers from 0.036 to 0.116 $(\mathrm{GeV/c})^2$. The electromagnetic form factor for these kaons is determined by

$$\mathrm{d}\sigma/\mathrm{d}q^2 = (\mathrm{d}\sigma/\mathrm{d}q^2)_{pt} \cdot |F_K(q^2)|^2$$

where the point cross section is, apart from radiative corrections

$$(\mathrm{d}\sigma/\mathrm{d}q^2)_{pt} = \frac{4\alpha^2}{q^4}(1 - q^2/q^2_{\max})$$

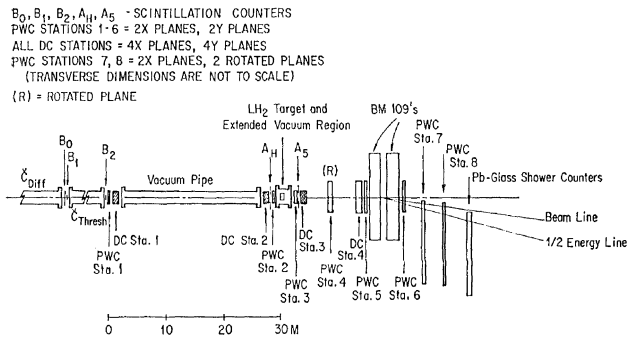

Fig. 1. High resolution single arm spectrometer.

The mean squared radius is determined by

$$\langle r_K^2 \rangle = -6|\mathrm{d}F_K(q^2)/\mathrm{d}q^2|_{q^2=0}$$

Elastic scatters were recorded by a high-resolution, single arm spectrometer which is illustrated in Fig. 1. The incident beam kaon and the scattered kaon and electron were tracked by both proportional wire chamber (PWC) stations and drift chamber (DC) stations.

Both chamber types were used in track finding and event recontruction to provide the high redundancy required for good efficiency. With PWC calibration an overall drift chamber resolution of approximately 100 *urn* was achieved and made possible good discrimination against the copious strong interaction background. The momentum of the scattered kaon and of the electron were determined by two magnets with a total field integral of 70.35 kg-m followed by three PWC stations. This was followed by a 21 radiation length lead-glass shower counter system which was used in the trigger and in the final background determination.

From the measured elastic scattering cross section and from the point cross section corrected to the measured electron energy, the form factor was determined as a function of the measured q^2. Our preliminary results are

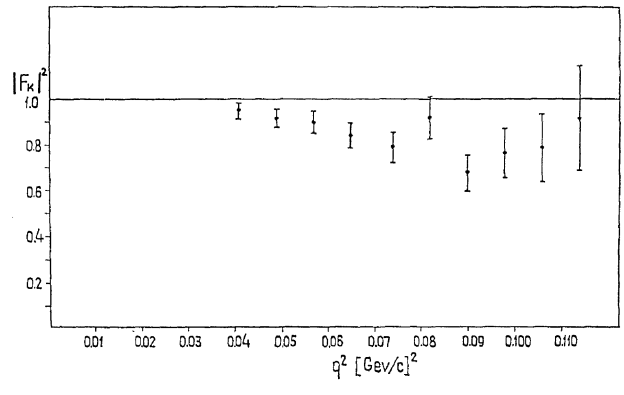

Fig. 2. Preliminary results on the kaon form factor as a function of q^2.

shown in Fig. 2. A fit to the dipole form gives <ri>=F0.26±0.07F^2 (or <rl:>$^{1/2}$-0.51± 0.07*F).* This may be compared to <rj?>= 0.31 ±0.04 F^2 (or <r*>$^{1/2}$=0.56±0.04 *F)* for the pion.[1] An accurate theoretical prediction has not been produced, but it is of interest to compare our result with the Chou-Yang model in which the kaon structure function is identified with the electromagnetic form factor. The model gives <r|$_c$>^{1}/^{2}=0.62 *F*\

We wish to express our gratitude to Professors R. R. Wilson and N. N. Bogolubov for their support of this form factor experiment and to thank the many of the Fermilab staff whose assistance made the success of this experiment possible.

References

1. E. Dally *et al:* Phys. Rev. Letters 39 (1977) 1176.
2. T.T.Chou: Phys. Rev. **Dll** (1975) 3145; A more recent analysis gives <r^^{2}>$^{1/2}$=-0.52±0.08 F (T.T. Chou, private communication).